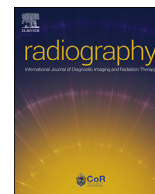




Since January 2020 Elsevier has created a COVID-19 resource centre with free information in English and Mandarin on the novel coronavirus COVID-19. The COVID-19 resource centre is hosted on Elsevier Connect, the company's public news and information website.

Elsevier hereby grants permission to make all its COVID-19-related research that is available on the COVID-19 resource centre - including this research content - immediately available in PubMed Central and other publicly funded repositories, such as the WHO COVID database with rights for unrestricted research re-use and analyses in any form or by any means with acknowledgement of the original source. These permissions are granted for free by Elsevier for as long as the COVID-19 resource centre remains active.



# Modifications to mobile chest radiography technique during the COVID-19 pandemic – implications of X-raying through side room windows

A. England<sup>a,\*</sup>, E. Littler<sup>b</sup>, S. Romani<sup>c</sup>, P. Cosson<sup>d</sup>

<sup>a</sup> School of Allied Health Professions, Keele University, Staffordshire, UK

<sup>b</sup> Department of Radiology, Warrington and Halton Teaching Hospitals NHS Foundation Trust, Warrington, UK

<sup>c</sup> LPD Lab Services, Blackburn, UK

<sup>d</sup> Medical Imaging Department, Teesside University, Middlesbrough, UK

## ARTICLE INFO

### Article history:

Received 29 June 2020

Received in revised form

21 July 2020

Accepted 23 July 2020

Available online 3 August 2020

### Keywords:

COVID-19

Mobile radiography

Modified technique

Image quality

Radiation dose

## ABSTRACT

**Introduction:** Modifications to common radiographic techniques have resulted from the challenges presented by the COVID-19 pandemic. Reports exist regarding the potential benefits of undertaking mobile radiography through side room windows. The aim of this study was to evaluate the impact on image quality and exposure factors when undertaking such examinations.

**Methods:** A phantom based study was undertaken using a digital X-ray room. Control acquisitions, using a commercially available image quality test tool, were performed using standard mobile chest radiography acquisition factors. Image quality (physical and visual), incidence surface air kerma (ISAK), Exposure Index (EI) and Deviation Index (DI) were recorded. Image quality and radiation dose were further assessed for two additional (experimental) scenarios, where a side room window was located immediately adjacent to the exit port of the light beam diaphragm. The goal of experimental scenario one was to modify exposure factors to maintain the control ISAK. The goal of experimental scenario two was to modify exposure factors to maintain the control EI and DI. Dose and image quality data were compared between the three scenarios.

**Results:** To maintain the pre-window (control) ISAK (76  $\mu$ Gy), tube output needed a three-fold increase (90 kV/4 mAs versus 90 kV/11.25 mAs). To maintain EI/DI a more modest increase in tube output was required (90 kV/8 mAs/ISAK 54  $\mu$ Gy). Physical and visual assessments of spatial resolution and signal-to-noise ratio were indifferent between the three scenarios. There was a slight statistically significant reduction in contrast-to-noise ratio when imaging through the glass window (2.3 versus 1.4 and 1.2;  $P = 0.005$ ).

**Conclusion:** Undertaking mobile X-ray examinations through side room windows is potentially feasible but does require an increase in tube output and is likely to be limited by minor reductions in image quality.

**Implications for practice:** Mobile examinations performed through side room windows should only be used in limited circumstances and future clinical evaluation of this technique is warranted.

© 2020 Published by Elsevier Ltd on behalf of The College of Radiographers.

## Introduction

The first description of human coronavirus, the family of viruses that now includes SARS-CoV-2, the cause of the current Covid-19 pandemic was published in The BMJ in 1965.<sup>1</sup> The majority of Covid-19 cases are either asymptomatic or result in only mild

disease.<sup>2</sup> However, in a substantial percentage of patients, a respiratory illness requiring hospitalisation develops.<sup>3</sup> Covid-19 has progressed rapidly and affected our daily lives to an extent not known in recent history.<sup>4</sup> Within the United Kingdom, as of 20th July 2020, there have been 294,792 cases and 45,312 deaths.<sup>5</sup>

Covid-19 is an aerosol transmissible disease that is thought to be transmitted by sneezing, coughing, and talking by an infected person.<sup>4</sup> Droplets can travel relatively long distances and can remain airborne for hours<sup>6</sup> or come to rest on a surface. Covid-19 is highly

\* Corresponding author. Mackay Building, School of Allied Health Professions, Keele University, Staffordshire, UK.

E-mail address: [a.England@keele.ac.uk](mailto:a.England@keele.ac.uk) (A. England).

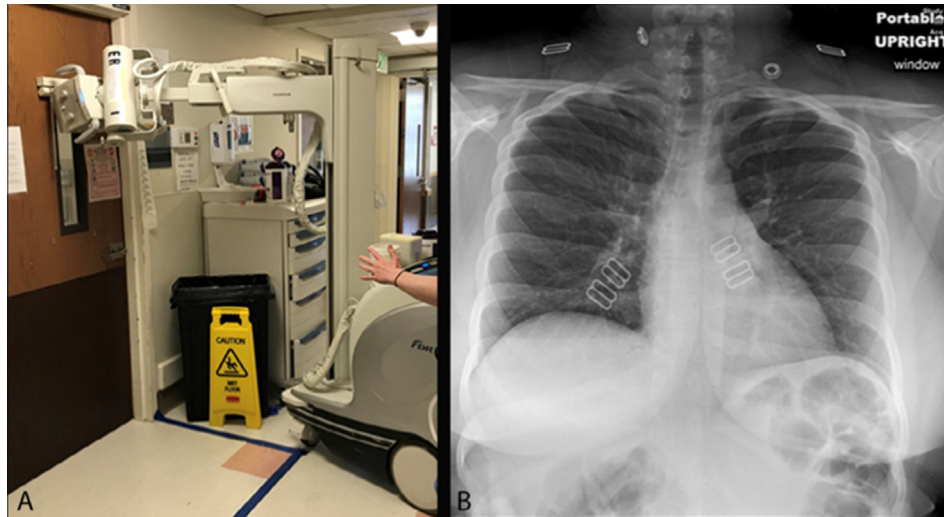


**Figure 1.** Example of a mobile CXR examination being undertaken through glass.<sup>1</sup> The mobile DR machine is positioned outside of the isolation (side) room, Image A. Image B demonstrates the resultant AP CXR image. Reproduced with permission from RSNA (images from Radiology).

contagious,<sup>4</sup> and there has not yet been any vaccine or effective treatment that has received regulatory approval.<sup>7</sup> Management of patients with known or suspected Covid-19 includes Medical Imaging (radiography and computed tomography (CT)).<sup>8</sup> As reported by Stogiannos and colleagues<sup>9</sup> practice varies widely within different countries, mainly due to differences in the access of resources (testing, imaging equipment, specialist staff and protective equipment).

Rapid human to human transfer has been widely confirmed<sup>10</sup> and healthcare professionals are at higher risk of catching the disease due to their exposure to higher viral loads.<sup>11</sup> In view of this, Zanardo and colleagues<sup>12</sup> based on their experiences in Italy, recommended that healthcare staff should take special precautions to limit cross-infection.

A number of institutions are reporting that in some instances mobile chest radiography is being undertaken through side room windows<sup>13,14</sup> in order to minimise the spread of the novel coronavirus SARS-CoV-2 (Fig. 1). Such practices are likely to provide additional opportunities for infection prevention but may also induce some limitations. Image quality degradation resulting from increased X-ray beam filtration, additional implications for radiation protection and increased wear and tear on the X-ray unit are just a few of the potential issues.

#### Aim

To evaluate the effect on image quality, radiation dose and tube life of undertaking X-ray examinations through glass side room windows.

#### Materials and methods

This experimental study was conducted using a commercially available fixed digital radiography (DR) unit with a similar specification to a digital mobile unit.<sup>15,16</sup> Images were subsequently acquired using a commercially available quality permission control test tool. As a result, ethics committee approval was not required but approval from the departmental manager was obtained.

#### Preliminary simulation

The experiment was at first simulated to provide starting values, to visualise the effect on the X-ray beam spectrum, and to estimate the

effect on the filament current thus ensuring no damage to the equipment was possible. TechnicVR v2.0 (Shaderware Ltd, UK) was used to provide the simulated data.

#### Imaging equipment and technique

Prior to commencing the study, quality assurance testing was undertaken in accordance with IPPEM Report 91<sup>17</sup>; results were within expected tolerances. A Samsung XGEO GC80 digital general radiography system (Samsung, Seoul, South Korea) together with a Caesium Iodide (CsI) AeroDR image detector (Konica Minolta Medical Imaging USA Inc, Wayne, NJ) was used.<sup>15</sup> The image receptor had an image capture area of 35 × 43 cm with a 2466 × 3040 pixel matrix, pixel size was 140 μm.

A Leeds Test Objects TOR 18FG (Leeds Test Objects, Leeds, UK) test tool was positioned erect 180 cm away from the X-ray tube focal spot (Fig. 2A). A fixed collimation field, at the detector surface, of 10 × 10 cm was applied. Collimation reflected the size of the test tool and it is acknowledged that it would be greater when undertaking chest radiography. The field size was restricted to the test tool in order to reflect normal radiographic practice of imaging the area under investigation. Beam centring was at the midpoint of the TOR 18FG test tool (Fig. 2B) and six degrees of caudal tube angulation was applied, as would typically be applied during erect anteroposterior chest radiography.<sup>18</sup>

An isolation/side room window was simulated using a double-glazed unit suitable for use as a door insert (Fig. 2C). The insert consisted of two panes of 4 mm tempered glass separated by a 30 mm void and could be used as a standard insert for a commercial interior door within a healthcare setting.<sup>19</sup>

The control series of acquisitions consisted of a fixed source-to-image distance (SID), filament size, tube potential and total filtration in keeping with mobile chest radiography. The tube charge was then selected to achieve an incident surface air kerma (ISAK) sufficient to report a zero-deviation index (DI). The experimental series of acquisitions included the glass window and an incremental increase in tube charge (mAs) was used to produce an ISAK equivalent to the control. The final experimental condition was a tube charge that resulted in a zero DI/equivalent EI to the control acquisitions.

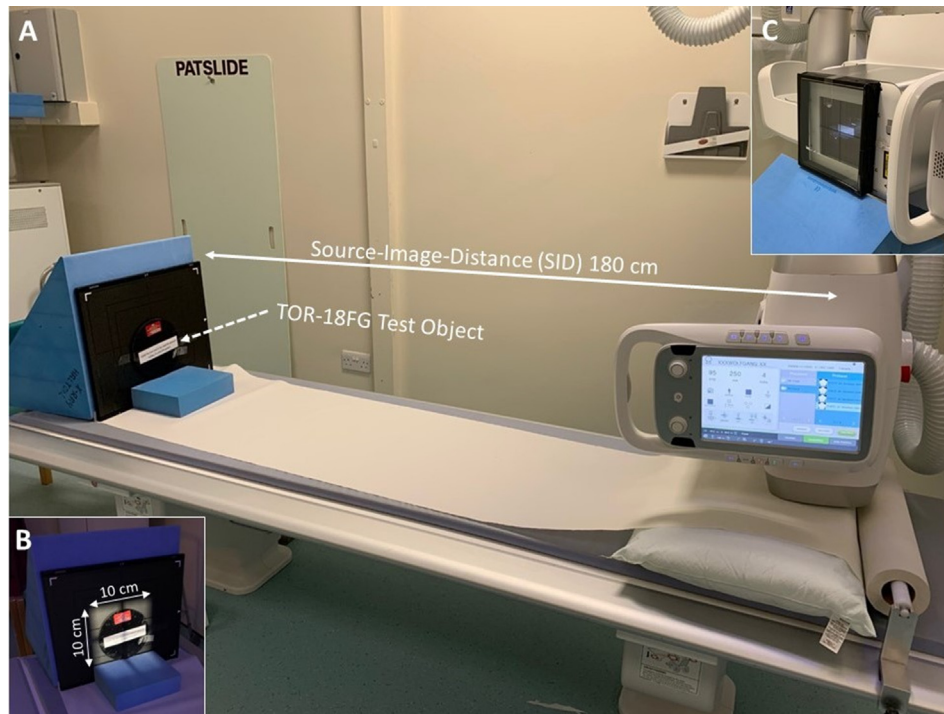


**Figure 2.** Experimental setup of the digital X-ray unit (A) and the TOR-18FG test object (B). For some acquisitions, a glass window unit (200 × 200 × 28 mm) was placed directly in contact with the exit port of the light beam diaphragm (C).

### Dosimetry

Three exposures were performed for each experimental setup. To minimise random errors from occurring, three exposures and three Dose Area Product (DAP), DI, Exposure Index (EI) and ISAK values were recorded.

### Image quality assessment

Both physical and visual grading of the resultant image quality was undertaken. Both methods used images displayed using a picture archiving and communication system (PACS) workstation (Carestream Vue PACS Version 12.2.2.1025, Carestream Health, Rochester, NY) and a 23 inch 2-megapixel colour monitor (Dell UZ2315H, Dell, Austin, TX). For each image the spatial resolution was determined together with the number of high contrast low detail discs visible on the image by a human observer. Observers were permitted to change the magnification and window levels in order to maximise visualisation, reflecting typical clinical processes of image interpretation. Observers consisted of two qualified radiographers with different levels of clinical experience (4–24 years). All observers were blinded to the image acquisition parameters, the presence or absence of the glass window and each other's observations. Room lighting was dimmed and reflected a typical radiology reporting room.

Signal to noise ratio (SNR) and contrast to noise ratio (CNR) have been successfully used as image quality metrics in a number of similar studies.<sup>20–23</sup> Four region of interests (ROIs) were drawn in homogeneous structures on the resultant test object images (Fig. 3). These were chosen to represent a range of low contrast details starting from the highest to the lowest and included the 7th and 11th discs. In order to sample the mean and standard deviation of the pixel values on the images software on the PACS workstation (Carestream Vue PACS) was used. SNR and CNR were calculated according to the following equations<sup>24,25</sup>:

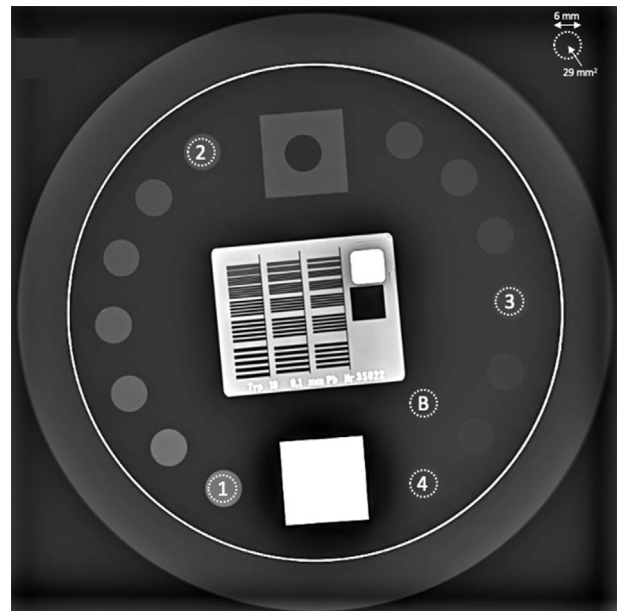


**Figure 3.** Resultant TOR-18FG test object image indicating the four ROI positions<sup>1–4</sup> and the location for measuring background signal and noise (B). All ROIs were located in the same position between measurements and had a diameter of 6 mm and an area of 29 mm<sup>2</sup>.

$$SNR = \frac{\text{mean signal}}{\sigma_{\text{noise}}}$$

$$CNR = \frac{ROI_X - ROI_B}{\sigma_2}$$

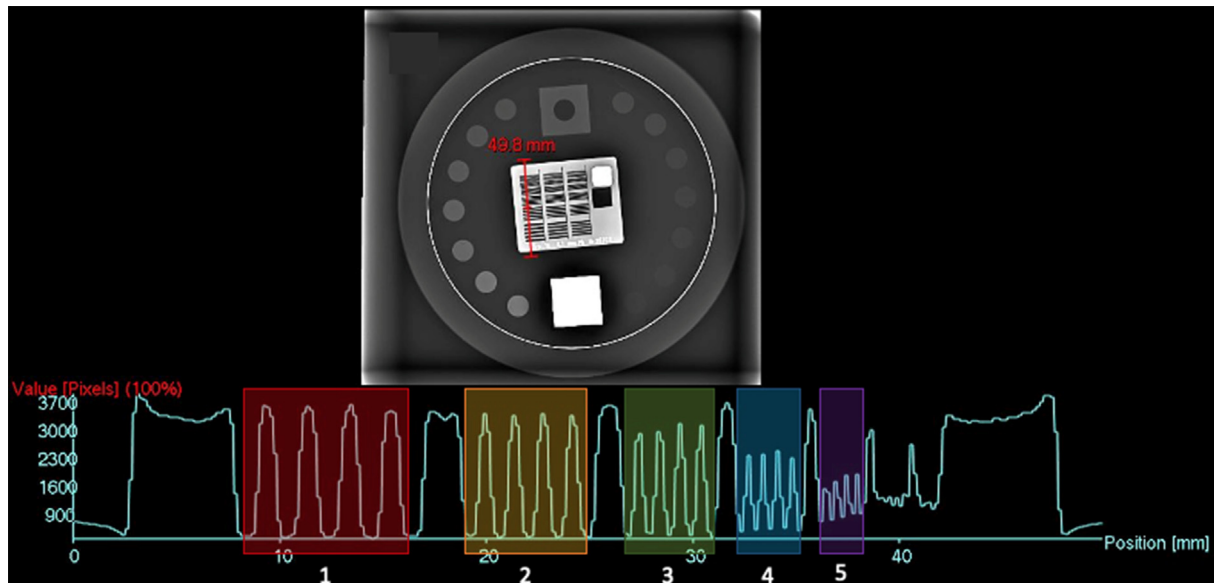


**Figure 4.** Resultant TOR-18FG test object image. A 50 mm straight line profile has been plotted across the first column of line pairs. Using the resultant histogram, the number of clear pairs of four lines are calculated. In this example, four groups of line pairs are visible where by four clear peaks and troughs were identifiable (coloured boxes).

where  $ROI_x$  is the mean signal from the area of interest (TOR contrast disc) and  $ROI_B$  is the mean signal from the background noise.  $\sigma_2$  was calculated as  $\sqrt{(SD1)^2 + (SD2)^2}/2$  where SD1 and SD2 are the standard deviations for  $ROI_x$  and  $ROI_B$ .

In terms of spatial resolution, the resultant image from the TOR-18FG test object was evaluated using three computer generated line profiles (Fig. 4). By summing the number of line pairs that were visible (four clear peaks and troughs on the histogram) the resolution of the image could be determined.

#### Statistical analysis

Data were inputted into Microsoft Excel (Microsoft Inc, Redmond, WA) and analysis was undertaken using the statistical programming package R. Normality of the data was confirmed visually and using the Shapiro–Wilk test ( $P > 0.05$ ). For each image acquisition a series of calculations were made for SNR, CNR and spatial resolution. Scenarios were compared using ANOVA and Tukey's HSD post-hoc analysis. Data were also summarised as a series of tables and graphs. P values of less than 0.05 were considered significant.

#### Results

Tube filtration was 3.5 mm Al, the focal spot size used was 1.2 mm<sup>2</sup>, no additional filtration was included, SID was 180 cm and tube voltage was 90 kV. For all acquisitions the target EI was 127. In the control condition (absence of the glass window), the tube charge necessary to generate a DI of zero was 4 mAs. This resulted in a mean (SD) ISAK and EI of 75.9 (0.2)  $\mu$ Gy and 128.0 (0.6), respectively.

The initial simulation using the same fixed exposure parameters and a tube charge of 4 mAs (achieved from a tube current of 250 mA and exposure time of 16 ms) resulted in an ISAK of 75.9  $\mu$ Gy and a Receptor Incident Air Kerma (RIAK) of 55.9  $\mu$ Gy (the TOR-18FG test object was substituted for 10 mm of polymethylmethacrylate and 0.1 mm of Al). The simulation generated an incident surface spectrum with an HVL of 4.6 mm Al. The filament current was 5.2 Amps

(Fig. 5). The simulation predicted a reduction in ISAK and RIAK to 35.2  $\mu$ Gy and 26.7  $\mu$ Gy respectively with the addition of 8 mm of glass (Fig. 5). To maintain a similar RIAK to the control with glass in the primary beam, the tube charge would need to increase to 8 mAs. This could either be achieved from a tube current of 250 mA and exposure time of 33 ms (filament current of 5.2 Amps), or from a tube current of 500 mA and an exposure time of 16 ms (filament current of 5.6 Amps). This X-ray beam, after transit through the glass, would have an HVL of 6.0 mm Al (Fig. 6).

In the empirical physical experiment, to maintain ISAK equivalence (76.3 [0.8]  $\mu$ Gy) when the glass window was added, the tube charge needed to be increased to 11.25 mAs, essentially a three-fold increase in output. For the experimental scenarios, when including the glass window and using 11.25 mAs, the mean (SD) ISAK and EI were 76.3 (0.8)  $\mu$ Gy and 182.0 (4.7), respectively. When aiming on maintaining a control 'zero DI', as with the original non-glass exposures, with the glass window in place required a tube charge of 8 mAs and this generated mean (SD) ISAK and EI of 53.7 (0.1)  $\mu$ Gy and 127.7 (3.1), respectively.

In terms of perceptual image quality, contrast sensitivity was not statistically different between the control and experimental acquisitions (14 versus 13 discs,  $P = 0.154$ ). This was also similar for the evaluation of spatial resolution between the control and experimental images (17 versus 16 line pairs,  $P = 0.540$ ).

For the physical evaluation of SNR, CNR and spatial resolution the data are summarised in Table 1. Using ANOVA there was a statistically significant difference in CNR values between scenarios ( $P = 0.005$ ). A post-hoc Tukey analysis revealed that there was a statistically significant difference between the control (no glass) and experimental scenario 2 (glass present, target ISAK) with  $P = 0.02$ . Differences between the control and experimental scenario 3 (glass present, target DI) was also statistically significant ( $P = 0.009$ ).

#### Discussion

The novel SARS-CoV-2 coronavirus has presented unprecedented challenges to imaging departments worldwide. One of the greatest challenges is that Covid-19 is extremely contagious and there are problems in preventing cross-infection for both patients

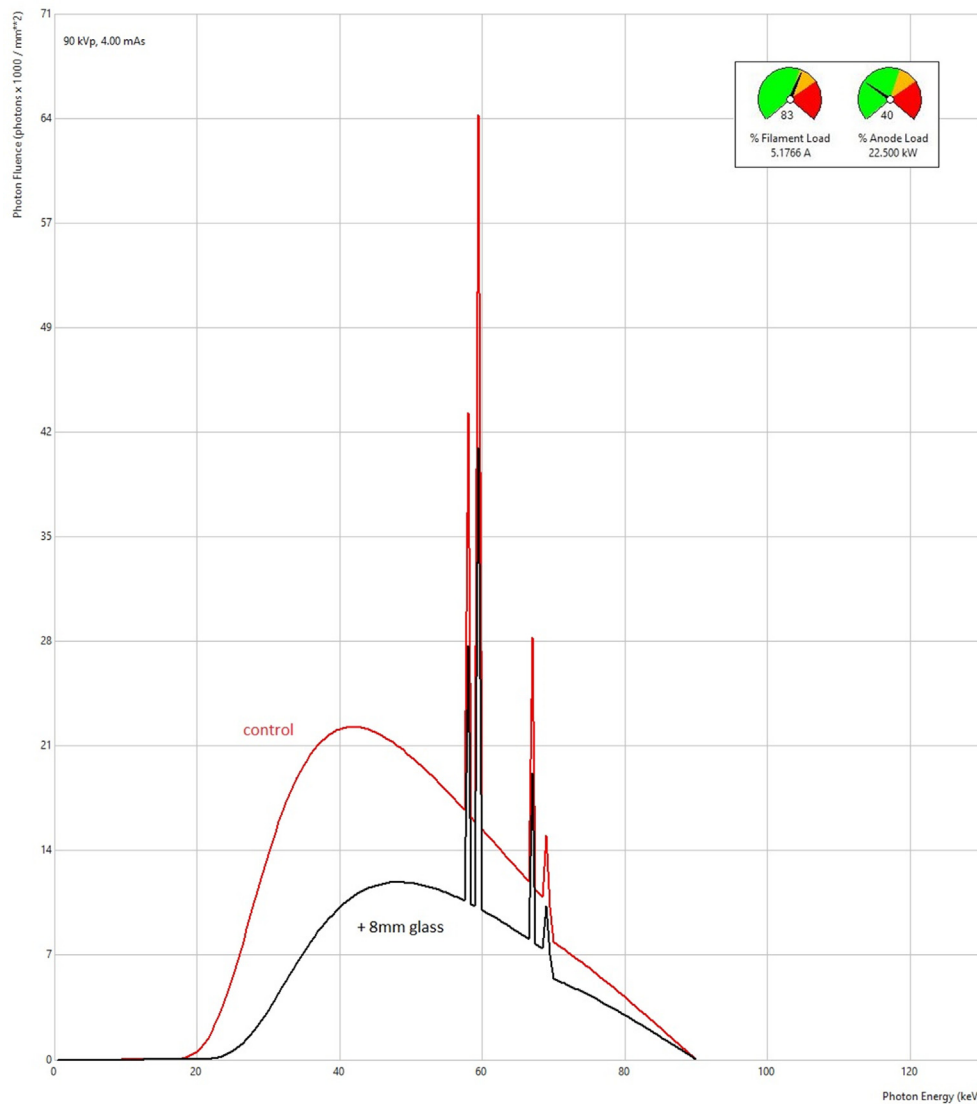


**Figure 5.** TechnicVR v2.0 (Shaderware Ltd, UK) simulation of the X-ray spectrum of the control beam (red line) and the required filament current (insert). The black line represents the beam attenuated by 8 mm of glass. (For interpretation of the references to color in this figure legend, the reader is referred to the Web version of this article.)

and hospital workers. It is not lost to anyone working in healthcare that there have been deaths reported in doctors, nurses and allied health professionals, including radiographers.<sup>26</sup> In view of this, new methods of working are essential in order to minimise disease transmission and protect both patients and staff members alike. Such processes are likely to be a balance of *risk vs risk* for practitioners and patients alike in contracting Covid-19. This can generate difficult dilemmas if there are multiple methods available for reducing risk for one group but not necessarily the other. In such a scenario, the question could arise as to where infection prevention priorities would focus.

As part of the early response to Covid-19 practitioners at the University of Washington, in the United States, reported on the option of imaging patients directly through glass windows in isolation/side rooms.<sup>13</sup> Advantages of this include not requiring the practitioner to directly attend the patient's bedside and not bringing the mobile X-ray unit in close proximity to the patient. An X-ray beam directed through a glass window would normally go against standard radiographic practices, in that exposure factors would need to be modified and that there could be artefacts and image quality issues arising from such techniques. Managing

Covid-19 will, however, require huge leaps of faith in how we modify our imaging practices to tackle these potential associated issues. It could be that such initiatives prove to be hugely beneficial in this fight, but at the same time they should still be subject to robust testing. Mossa-Basha and colleagues<sup>13</sup> describe imaging through side room windows, and state that there were no obvious image quality issues. Their publication sought to describe rapid and widespread changes to their operating practices in response to Covid-19, it is likely that image quality was not subject to the usual standard of rigorous objective testing.

Based on our initial work it can be concluded that on the basis of visual inspection, there does not appear to be any significant detriment from imaging through a glass window unit. To maintain either equivocal DI or ISAK/RIAK, the exposure factors would need to be increased by two to three-fold. This will have implications on either the wear and tear of X-ray equipment (increase in filament current) or decrease in temporal resolution (increase in exposure time) depending on how the extra charge (mAs) is generated (increased filament current or time). The inclusion of a glass window within the primary beam 'hardens the beam' as seen in Figs. 5 and 6. The reduction in low energy photons leads to a beam with a

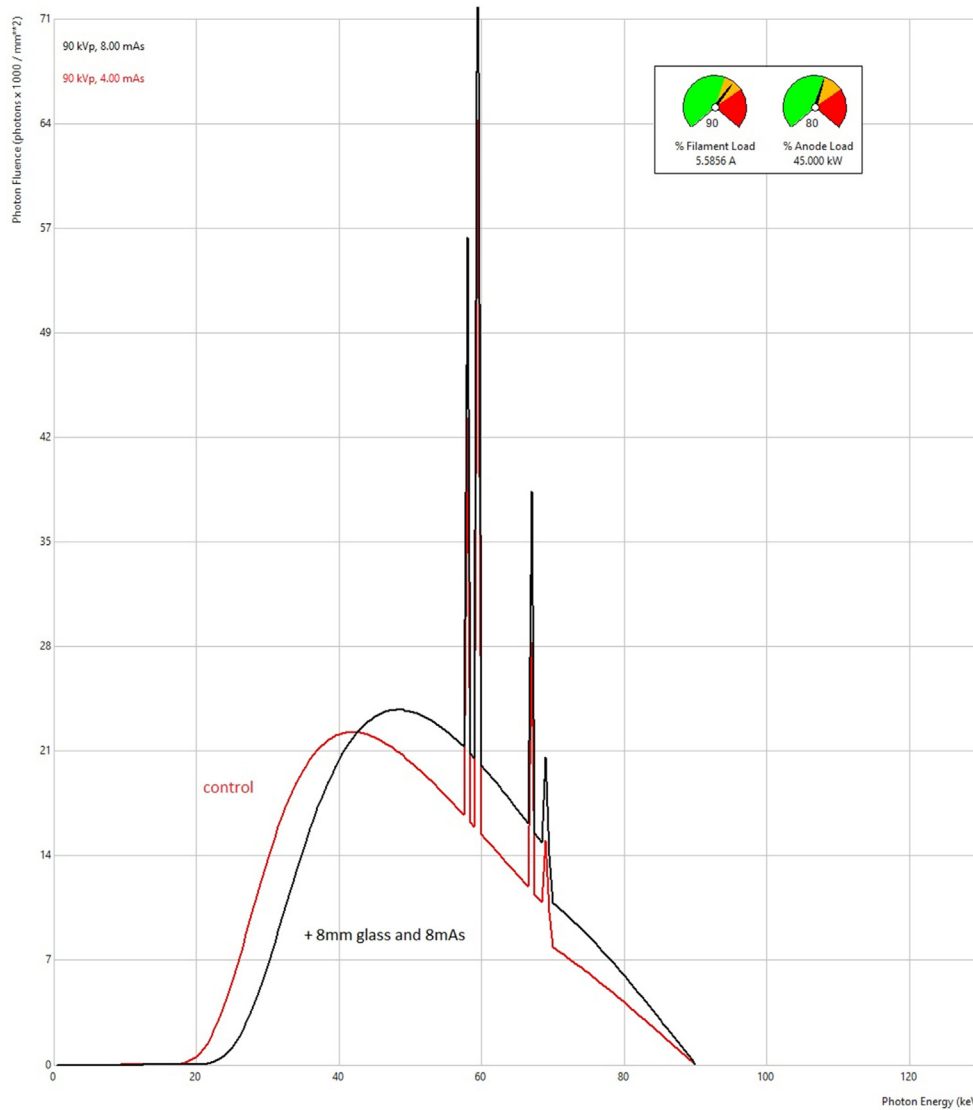


**Figure 6.** TechnicVR v2.0 (Shaderware Ltd, UK) simulation of the X-ray spectrum of the control beam (red line) and the experimental (black line) scenario, with increased tube charge to compensate for glass. (For interpretation of the references to color in this figure legend, the reader is referred to the Web version of this article.)

**Table 1**  
A summary of SNR, CNR and spatial resolution results for the different scenarios.

Scenario	Target	Mean (SD)		Spatial resolution (LP/mm)
		SNR	CNR <sup>a</sup>	
1 – no glass		35.5 (2.7)	2.3 (0.2)	2.24
2 – glass present	ISAK	39.6 (2.4)	1.4 (0.2)	2.50
3 – glass present	DI	37.0 (4.1)	1.2 (0.4)	2.24

<sup>a</sup> ANOVA, P = 0.005.

higher effective photon energy. This is likely to reduce image contrast, and this was demonstrated in the physical calculations (Table 1). There were no significant differences in the physical measures of SNR but there was a significant, but small, reduction in CNR when imaging through the glass window. Based on the perceptual analysis this difference was not apparent to the observers. Multiple reasons could be suggested for this, physical CNR values are much more sensitive to changes in image quality than visual inspections.<sup>27</sup>

This result, taken together with the possibility of reduction in temporal resolution due to the beating heart, could suggest in some instances, very subtle pathology could potentially be missed when modifying mobile imaging protocols. Many would argue that there are specific reasons for undertaking mobile radiography and that further imaging is likely when a patient's condition improves, either prior to discharge or during follow up. This however may not be the case for all patients and clinicians should be aware of the potential limitations when reviewing an X-ray image acquired through glass; as a minimum the resultant image should be annotated to reflect the modified technique. However, it is highly likely that the identification of subtle detail/changes in a background of Covid-19 is important. Covid-19 commonly affects the peripheral and lower lung zones bilaterally<sup>28</sup> and thus the assessment of airspace shadowing across the whole lung fields is paramount. In support of this Sim et al.<sup>29</sup> argue that since Covid-19 appearances may be subtle, high image quality is required from mobile X-ray units. Such challenges have been further reported in a series of publications highlighting patients who had normal CXR appearances and who went on to subsequently have ground glass opacifications demonstrated on CT.<sup>8,30</sup>

Even for an erect patient, it is common to apply a small caudal angulation to an AP projection of the chest so that the central ray is perpendicular to the long axis of the sternum. This is to ensure the clavicles do not obscure the apices of the lungs.<sup>31</sup> If the patient is able to sit up erect, when using a SID of 180 cm, then this would require the center of the receptor to be approximately 20 cm below the point through which the central ray passed through the window. It can be seen that once the patient is so ill that they can only achieve a semi erect position, then a tube angulation typically of 30° would be required. This would necessitate a height difference of 1 m between the centre of the receptor and the point through which the central ray passed through the window. Since most door windows are below 180 cm in height, this will require a trolley that is able to be lowered to 80 cm from the floor or even less and would remain an important technical consideration.

X-raying through side room windows could have wider applicability in other areas of clinical practice where infection control is paramount. Imaging following stem cell transplantation, suspected or known cases of MRSA and clostridium difficile, to name but a few could benefit from a similar approach. Indeed, the work originally described using a similar technique by the University of Washington stemmed from the imaging of suspected Ebola virus patients in Africa.<sup>32</sup>

Within our work, we presented the results of a novel experiment which sought to provide initial image quality and dose data regarding the practice of X-ray imaging through glass windows. Our response to modified Covid-19 radiographic techniques needed to be rapid and as such there were many additional elements to this study which could have been included. We did, however, opt to present some initial data regarding the feasibility of this technique within other areas of practice. We do, however, agree that more work should be undertaken, including clinical analyses using dedicated mobile equipment, before either confirming or refuting this practice definitively. It should also be noted that the technical options for including glass within interior doors is vast.<sup>19</sup> The exact specification of the glazed unit can vary within an institution and will have some dependency on the location and purpose of the door, installation date and building control regulations within each country. Further research should be undertaken to understand the influence of different types of glass inserts.

## Conclusion

The response of radiology practitioners to the Covid-19 pandemic has been immense. Many new techniques and breakthroughs will result from the new knowledge and experiences gained during this time. New approaches to imaging should be carefully considered and evaluated in order to provide optimum care and safety to both staff and patients. Based on data reported with our work it does appear feasible for mobile radiography to be undertaken through side room windows in specific instances. With the potential for increases in tube output and reductions in image quality this technique should only be used when other options are not feasible, and clinicians should be aware of any modifications to standard techniques. Practitioners should also be mindful that such modifications would require additional training.

## Conflict of interest statement

None.

## Acknowledgement

No funding was provided for this study.

## References

- Mahase E. Covid-19: coronavirus was first described in. *BMJ* 2020;**369**:m1547.
- Horby P, Lim WS, Emberson JR, Mafham M, Bell JL, Linsell L, et al. Dexamethasone in hospitalized patients with Covid-19 - preliminary report. *N Engl J Med* 2020. <https://doi.org/10.1056/NEJMoa2021436>.
- Verity R, Okell LC, Dorigatti I, Winskill P, Whittaker C, Imai N, et al. Estimates of the severity of coronavirus disease 2019: a model-based analysis. *Lancet Infect Dis* 2020;**20**(6):669–77.
- Schröder I. COVID-19: a risk assessment perspective. *ACS Chem Health Saf* 2020;**27**(3):160–9.
- Roser M, Ritchie H, Ortiz-Ospina E, Hasell J. *Coronavirus pandemic (COVID-19): OurWorldInData.org*. <https://ourworldindata.org/coronavirus>; 2020.
- van Doremalen N, Bushmaker T, Morris DH, Holbrook MG, Gamble A, Williamson BN, et al. Aerosol and surface stability of SARS-CoV-2 as compared with SARS-CoV-1. *N Engl J Med* 2020;**382**(16):1564–7.
- Lotfi M, Hamblin MR, Rezaei N. COVID-19: transmission, prevention, and potential therapeutic opportunities. *Clin Chim Acta* 2020;**508**:254–66.
- Cellina M, Orsi M, Toluian T, Valenti Pittino C, Oliva G. False negative chest X-Rays in patients affected by COVID-19 pneumonia and corresponding chest CT findings. *Radiography* 2020;**26**(3):e189–94.
- Stogiannos N, Fotopoulos D, Woznitza N, Malamateniou C. COVID-19 in the radiology department: what radiographers need to know. *Radiography* 2020;**26**(3):254–63.
- Shereen MA, Khan S, Kazmi A, Bashir N, Siddique R. COVID-19 infection: origin, transmission, and characteristics of human coronaviruses. *J Adv Res* 2020;**24**:91–8.
- Burdorf A, Porru F, Rugulies R. The COVID-19 (Coronavirus) pandemic: consequences for occupational health. *Scand J Work Environ Health* 2020;**46**(3):229–30.
- Zanardo M, Martini C, Monti CB, Cattaneo F, Ciaralli C, Cornacchione P, et al. Management of patients with suspected or confirmed COVID-19, in the radiology department. *Radiography* 2020;**26**(3):264–8.
- Mossa-Basha M, Medverd J, Linnau K, Lynch JB, Wener MH, Kicska G, et al. *Policies and guidelines for COVID-19 preparedness: experiences from the university of Washington*. *Radiology*. 2020. p. 201326.
- Sng LH, Arlany L, Toh LC, Loo TY, Ilzam NS, Wong BSS, et al. Initial data from an experiment to implement a safe procedure to perform PA erect chest radiographs for COVID-19 patients with a mobile radiographic system in a “clean” zone of the hospital ward. *Radiography* 2021;**27**(1):48–53. <https://doi.org/10.1016/j.radi.2020.05.011>.
- Electronics S. *Samsung XGEO GC80: Samsung electronics*. 2013. [http://www.flexomedical.it/wp-content/uploads/2017/05/samsung\\_xgeo\\_gc80.pdf](http://www.flexomedical.it/wp-content/uploads/2017/05/samsung_xgeo_gc80.pdf).
- Carestream. *DRX-revolution mobile X-ray system*. Carestream; 2020.
- Recommended standards for the routine performance testing of diagnostic X-ray imaging systems*. York: Institute of Physics and Engineering in Medicine; 2005.
- Whitley AS, Clark KC. *Pir. Clark's positioning in radiography*. London: Hodder Arnold; 2005.
- Hormann Doors for Healthcare Systems. *All-in-one specialist solutions*. [https://www.hormann.kr/fileadmin/\\_country/hoermann.cn/kataloge/HCR-EN.pdf](https://www.hormann.kr/fileadmin/_country/hoermann.cn/kataloge/HCR-EN.pdf); 2020.
- Sandborg M, Tingberg A, Ullman G, Dance DR, Alm Carlsson G. Comparison of clinical and physical measures of image quality in chest and pelvis computed radiography at different tube voltages. *Med Phys* 2006;**33**(11):4169–75.
- Hess R, Neitzel U. Optimizing image quality and dose for digital radiography of distal pediatric extremities using the contrast-to-noise ratio. *Röfo* 2012;**184**(7):643–9.
- Martin C. Optimisation in general radiography. *Biomed Imaging Interv* 2007;**3**:e18.
- Mori M, Imai K, Ikeda M, Iida Y, Ito F, Yoneda K, et al. Method of measuring contrast-to-noise ratio (CNR) in nonuniform image area in digital radiography. *Electron Commun Jpn* 2013;**96**(7):32–41.
- Inoue K, Kise K. Analysis of the effect of dataset differences on object recognition: the case of recognition methods based on exact matching of feature vectors. *Electron Commun Jpn* 2013;**96**(9):33–45.
- Alves AF, Alvarez M, Ribeiro SM, Duarte SB, Miranda JR, Pina DR. Association between subjective evaluation and physical parameters for radiographic images optimization. *Phys Med* 2016;**32**(1):123–32.
- Lapolla P, Mingoli A, Lee R. Deaths from COVID-19 in healthcare workers in Italy—What can we learn? *Infect Control Hosp Epidemiol* 2020:1–2.
- Tapiovaara MJ. Review of relationships between physical measurements and user evaluation of image quality. *Radiat Protect Dosim* 2008;**129**(1–3):244–8.
- Woznitza N, Nair A, Hare SS. COVID-19: a case series to support radiographer preliminary clinical evaluation. *Radiography* 2020;**26**(3):e186–8.
- Sim WY, Chen RC, Aw LP, Abu Bakar R, Tan CC, Heng AL, et al. How to safely and sustainably reorganise a large general radiography service facing the COVID-19 pandemic. *Radiography* 2020 Nov;**26**(4):e303–11.
- Jacobi A, Chung M, Bernheim A, Eber C. Portable chest X-ray in coronavirus disease-19 (COVID-19): a pictorial review. *Clin Imag* 2020;**64**:35–42.
- Bontrager KL, Lampignano JP. In: Bontrager Kenneth L, Lampignano John P, editors. *Textbook of radiographic positioning and related anatomy*. 6th ed. St. Louis, Mo.; [London]: Elsevier Mosby; 2005.
- Auffermann WF, Kraft CS, Vanairsdale S, Lyon GM, Tridandapani S. Radiographic imaging for patients with contagious infectious diseases: how to acquire chest radiographs of patients infected with the Ebola virus. *Am J Roentgenol* 2014;**204**(1):44–8.